
Original Paper

Effects of Misalignment of High Speed Flexible Coupling on the Fighter Aircraft Transmission Characteristics

Nagesh Samikkanu and Abu Muhammed Junaid Basha

Combat Vehicles Research and Development Establishment,
Avadi, Chennai 600 054, India
nge0207@gmail.com

Abstract

The Fighter aircraft transmission system consists of a light weight, High Speed Flexible Coupling (HSFC) known as Power Take-Off shaft (PTO) for connecting Engine gearbox (EGB) with Accessory Gear Box (AGB). The HSFC transmits the power through series of specially contoured metallic annular thin flexible plates whose planes are normal to the torque axis. The HSFC operates at high speed ranging from 10,000 to 18,000 rpm. The HSFC is also catered for accommodating larger lateral and axial misalignment resulting from differential thermal expansion of the aircraft engine and mounting arrangement. The contoured titanium alloy flexible plates are designed with a thin cross sectional profile to accommodate axial and parallel misalignment by the elastic material flexure. This paper investigates the effect of misalignment on the transmission characteristics of the HSFC couplings. A mathematical model for the HSFC coupling with misalignment has been developed for analyzing the torque transmission and force interaction characteristics. An extensive testing has been conducted for validating characteristics of the designed coupling under various misalignment conditions. With this the suitability of the model adapted for the design iteration of HSFC development is validated. This method will reduce the design iteration cycles of HSFC and can be extended for the similar development of flexible couplings.

Keywords: Flexible Couplings, Misalignment, rotor dynamics, system dynamics and simulation, Experimental validation, Failure Prevention.

1. Introduction

The Fighter aircraft transmission system consists of a light weight, High Speed Flexible Coupling (HSFC) known as power take-off shaft for connecting Engine gearbox (EGB) with Accessory Gear Box (AGB). The HSFC transmits the power through series of specially contoured metallic annular thin flexible plates whose planes are normal to the torque axis as shown in Fig 1. The HSFC operates at high speed ranging from 10,000 to 18,000 rpm from the EGB to AGB. The HSFC also catered for accommodating larger angular and axial misalignment resulting from differential thermal expansion of the aircraft engine and mounting arrangement. The contoured titanium alloy flexible plates are designed with a thin cross sectional profile to accommodate axial and parallel misalignment by the elastic material flexure. The parallel misalignment and axial displacement distorts or bends the flexible plates which are designed with thinner cross section to maintain lower bending and axial stresses for a given torque capacity. Due to misalignment, the HSFC is subjected to high cyclic stresses. The present work investigates the effect of misalignment of the HSFC on the Fighter Aircraft Transmission Characteristics. The mathematical model for the HSFC coupling with misalignment is constructed for the purpose of deriving the equations governing the torque transmission and force interaction characteristics. The test apparatus is constructed for verifying the static and dynamic characteristics of the designed coupling under various misalignment conditions. Good agreement between numerical simulation and experimental results is obtained are presented.

1.1 Configuration of HSFC

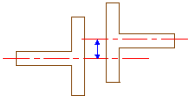
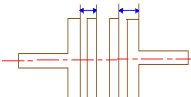
The schematic view of the High speed flexible coupling is depicted in Figure 1. The flexible plate cross sectional profile may be straight, contoured, tapered or convoluted. The flexible plate used for HSFC designed to suit the operating conditions, misalignment requirements, enveloping dimensional restrictions and safety [1]. The size of the coupling is based on the mean and maximum operation torques. The imposed axial, parallel and rotational misalignments resulting in enhanced stress level on the

flexible plates. These are investigated and confirmed by extensive static and dynamic stress analysis. Two flexible plate packs assembled in the input and output end of HSFC connected by a centre tube to share the loads equally during operating condition.

1.2 HSFC Misalignment

The HSFC misalignment occurs when the centerlines of rotation of two power transmitting shafts are not in line with each other. The misalignment is the deviation of relative shaft position from a collinear axis of rotation, measured at the point of rotation [2]. The misalignment may result in excessive vibrations [3]. In the aircraft transmission system, as the engine and accessories drives are mounted on different bases, the dynamic operating conditions results in parallel misalignment of HSFC. The axial misalignment of the HSFC is due to the thermal expansion of engine during operation. The HSFC transmits torque through a stack of thin metal flexible plates. The free span of the flexible plates deflects to accommodate angular misalignment and allow minor axial shaft movement. The HSFC misalignment [3] occurs when the centerlines of rotation of two power transmitting shafts are not in line with each other. The misalignment is the deviation of relative shaft position from a collinear axis of rotation (measured at the points of rotation). The coupling misalignment conditions are shown in Table 1.

Table 1 Coupling Misalignment

Sl. No	Misalignment	Misalignment Condition
1	In parallel misalignment the two axes are parallel but at a relatively small distance apart.	
2	In axial misalignment shafts are positioned at the same axis but separated by a small distance.	

In the aircraft transmission system as the engine drives and accessories drive are mounted on different bases, the dynamic operating conditions result in parallel misalignment of HSFC. The axial misalignment of the HSFC is due to the thermal expansion of engine during operation.

2. Influence of Articulation length on parallel Misalignment

The configuration of HSFC is shown in Fig 1. The flexible plates pack accommodates the misalignment imposed on the system. The articulation length is the distance between the center of flexible plate packs attached at either end of the center tube. The Fig 2 shows articulation length of HSFC. The location of flexible plates packs influences the amount of misalignment it can accommodate.

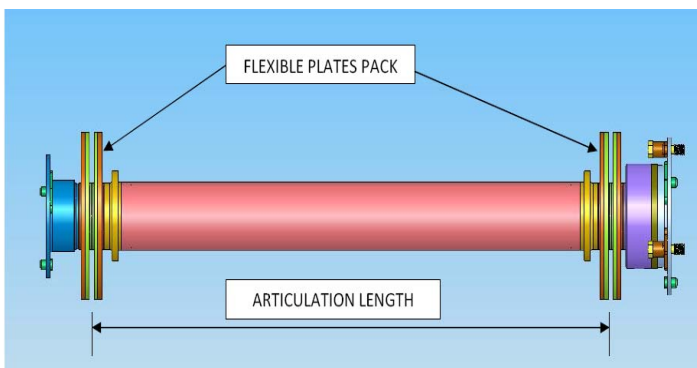


Fig. 1 Configuration of HSFC

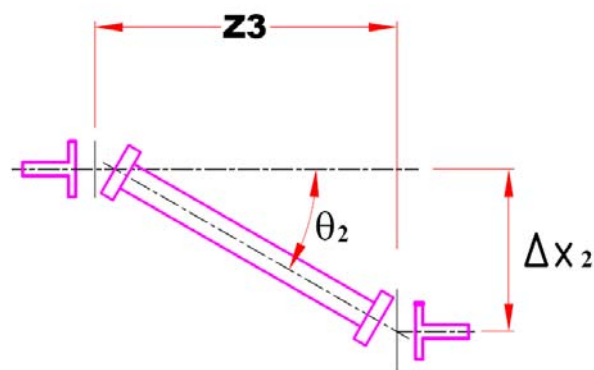


Fig. 2 Articulation length (Z_3) of HSFC

The relation between the off- set distance and articulation length is given by the eq (1).

$$\Delta X_2 = \tan(\theta_2) \cdot Z_3 \tag{1}$$

In case of axial misalignment the articulation length has no influence on the amount of misalignment. But in case of Parallel misalignment the articulation length determines the magnitude of parallel misalignment distance. The table 2 shows the rotating angle and offset distance with various articulation lengths.

Table 2 Influence of articulation length of HSFC

Rotating angle (θ_2)	Articulation length, Z_3 (mm)			
	350	400	425	450
	Resulting Off set distance (mm)			
0.5	3.052739	3.488845	3.706897	3.92495
1.0	6.105246	6.977424	7.413513	7.849602
1.5	9.157288	10.46547	11.11956	11.77366
2.0	12.20863	13.95272	14.82477	15.69682
2.5	15.25905	17.43892	18.52885	19.61878
3.0	18.30831	20.92378	22.23152	23.53925
3.5	21.35617	24.40705	25.93249	27.45793
4.0	24.40241	27.88847	29.6315	31.37453
4.5	27.44679	31.36776	33.32825	35.28873
5.0	30.48908	34.84467	37.02246	39.20025

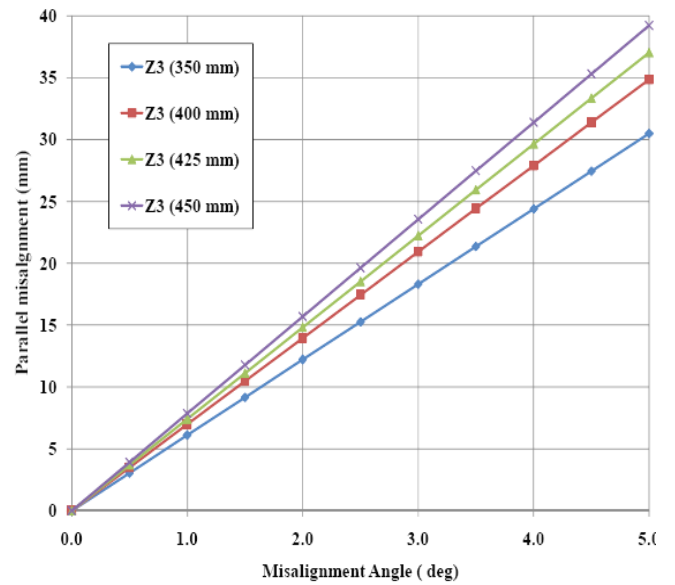


Fig. 3 Influence of articulation length

The typical case with rotating angle of 1.5° the increase in resulting off-set distance for the articulation length of 450 mm is 22.2 % more when compared to 350 mm of articulation length. So, for the same rotating angle (θ_2), increase in articulation length (Z_3) resulting in increase in resulting off-set distance which is to be accommodated by the HSFC. With the lower rotating angle (θ_2), the corresponding bending stress induced on the flexible elements will be less thereby increase in the HSFC service life can be realized.

3. Coupling Misalignment

The reaction forces and moments developed due to parallel Misalignment has been analysed by Gibbons [4]. The rotor bearing system has been modelled and the reaction forces, moments developed due to flexible coupling misalignment are derived by A. S Sekhar and B. S Prabhu [5]. With these, in the present study, the reaction forces, moments developed due to HSFC misalignment is arrived. The coordinates of parallel misalignment of HSFC is shown in Fig 4. During parallel misalignment the centre-lines Z_1 and Z_2 are misaligned. The torque is applied at input end and that the rotation is in the same direction as the applied torque. The reaction forces and moments which the HSFC exerts on the end supports are as given below.

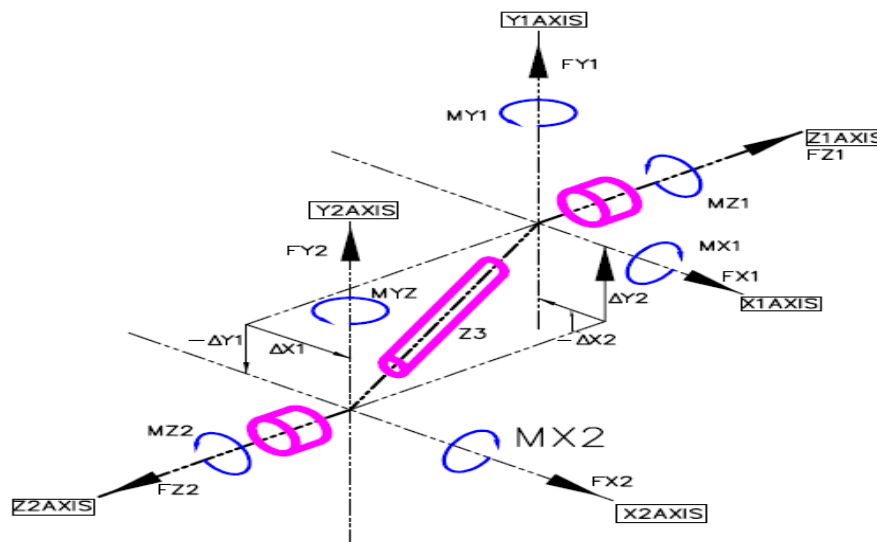


Fig. 4 Coordinates of parallel misalignment of HSFC

The centre-line of the center tube, a coupling spacer is connecting the HSFC centerlines, with intersection points on the coupling articulation center. The values and the directions of displacements, ΔX_2 and ΔY_2 can be substituted to simulate the misalignment. Assuming that Z_1 is the axis of driving end and the torque is applied as shown in Fig 4 where the rotation is in the same direction as the applied torque, the reaction forces and moments that the coupling exerts on the end supports are arrived from the system equation of motion of HSFC.

3.1 Equation of motion of HSFC

The following are reaction forces & moments that are developed on account of parallel misalignment

$$MX_1 = T_q \sin\theta_1 + K_b \Phi_1 \quad (2)$$

$$MY_1 = T_q \sin\Phi_1 - K_b \theta_1 \quad (3)$$

$$MX_2 = T_q \sin\theta_2 - K_b \Phi_2 \quad (4)$$

$$MY_2 = T_q \sin\Phi_2 + K_b \theta_2 \quad (5)$$

$$FX_1 = \frac{-MY_2 - MY_1}{Z_B} \quad (6)$$

$$FY_1 = \frac{-MX_2 + MX_1}{Z_B} \quad (7)$$

$$FZ_1 = Ka \Delta Z + Ka (\Delta Z)^3 \quad (8)$$

$$\theta_1 = \sin^{-1} \left(\frac{\Delta X_1}{Z_B} \right) \quad (9)$$

$$\theta_2 = \sin^{-1} \left(\frac{\Delta X_2}{Z_B} \right) \quad (10)$$

$$\Phi_1 = \sin^{-1} \left(\frac{\Delta Y_1}{Z_B} \right) \quad (11)$$

$$\Phi_2 = \sin^{-1} \left(\frac{\Delta Y_2}{Z_B} \right) \quad (12)$$

Considering the linear bending and axial spring rates for the HSFC are assumed. Therefore,

$$FX_2 = -FX_1 \quad (13)$$

$$FY_2 = -FY_1 \quad (14)$$

$$FZ_2 = FZ_1 \quad (15)$$

From these forces in each direction can be obtained. For the design iteration of HSFC, initial guess value can be substituted for comparative calculations. Thus the reaction forces and moments can be calculated by considering system equation of motion.

3.2 Bending stiffness Vs Forces and moments

In this the articulation length and induced torques are kept constant and the bending stiffness of the HSFC is varied to study the resulting forces and moments. The bending stiffness also influences the bending natural frequency of the HSFC [6]. The results are shown in Table 3.

Table 3 Variation in Bending stiffness Vs Forces and moments

Torque (Tq)	k _b	Mx ₁	My ₁	Mx ₂	My ₂	FX ₁	FY ₁	ΔX ₂	ΔY ₂	Z ₃
100	0	0	0.0000	2.8235	2.8235	-0.0066	0.0066	12	12	425
100	950	0	0.0000	-24.0036	29.651	-0.0698	-0.0565	12	12	425
100	1900	0	0.0000	-50.8307	56.478	-0.1329	-0.1196	12	12	425
100	2850	0	0.0000	-77.6578	83.305	-0.1960	-0.1827	12	12	425
100	3325	0	0.0000	-91.0713	96.718	-0.2276	-0.2143	12	12	425
100	4750	0	0.0000	-131.3119	136.96	-0.3223	-0.3090	12	12	425

As the bending stiffness increases the corresponding moment and forces on the end support are increasing. The bending stiffness variation Vs moments and bending stiffness Vs forces are shown in Fig 5 & 6.

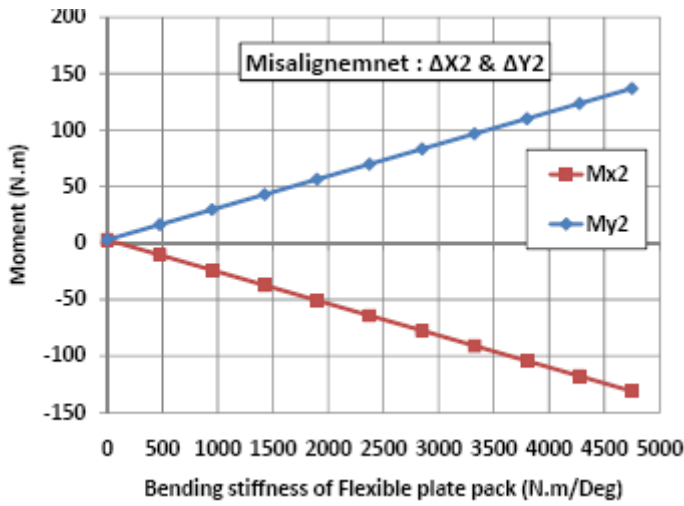


Fig 5. Bending stiffness Vs end moments

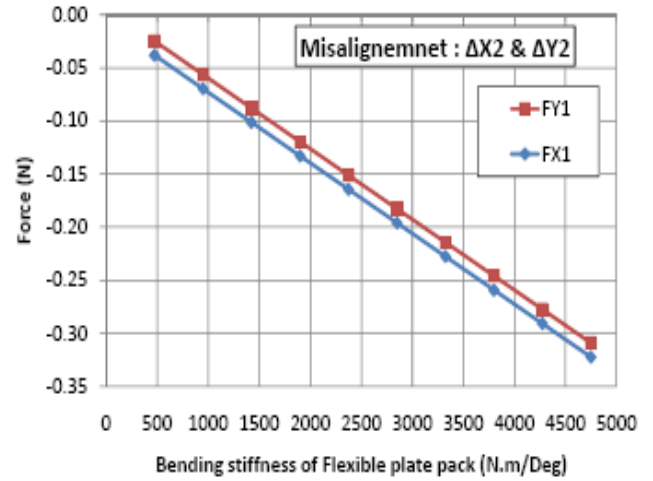


Fig 6. Bending stiffness Vs Forces

3.3 Articulation length Vs Forces and moments

In this the induced Torque and bending stiffness is kept constant and articulation length of the HSFC is varied. The resulting forces and moments are calculated for the typical HSFC are given in Table 4. The articulation length Vs end moments and articulation length Vs reaction forces are shown in Fig 7 & 8.

Table 4 Articulation length Vs Forces and end moments

Torque (Tq)	K_b	M_{x_2}	M_{y_2}	F_{X_1}	F_{Y_1}	ΔX_2	ΔY_2	Z_3
100	4.75E+03	-186.0507	194.051	-0.64684	-0.6202	12	12	300
100	4.75E+03	-171.7322	179.117	-0.55113	-0.5284	12	12	325
100	4.75E+03	-159.4605	166.318	-0.47519	-0.4556	12	12	350
100	4.75E+03	-148.8260	155.226	-0.41394	-0.3969	12	12	375
100	4.75E+03	-139.5214	145.521	-0.36380	-0.3488	12	12	400
100	4.75E+03	-131.3119	136.959	-0.32226	-0.3090	12	12	425
100	4.75E+03	-124.0150	129.348	-0.28744	-0.2756	12	12	450
100	4.75E+03	-117.4865	122.539	-0.25798	-0.2473	12	12	475

As the articulation length increases the corresponding moment and forces on the end support are decreasing. It will be advantageous to have more articulation length to reduce the end moments and forces as shown in the articulation length Vs end moments and articulation length Vs forces as shown in Fig 7 & 8.

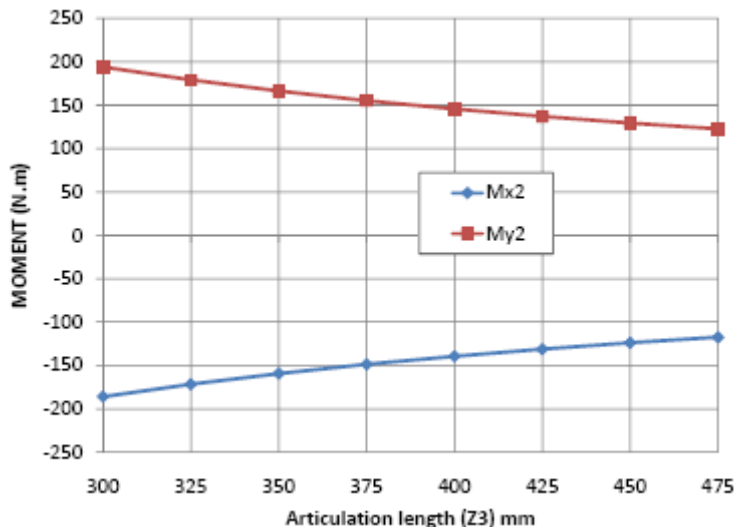


Fig 7. Articulation length Vs end moments

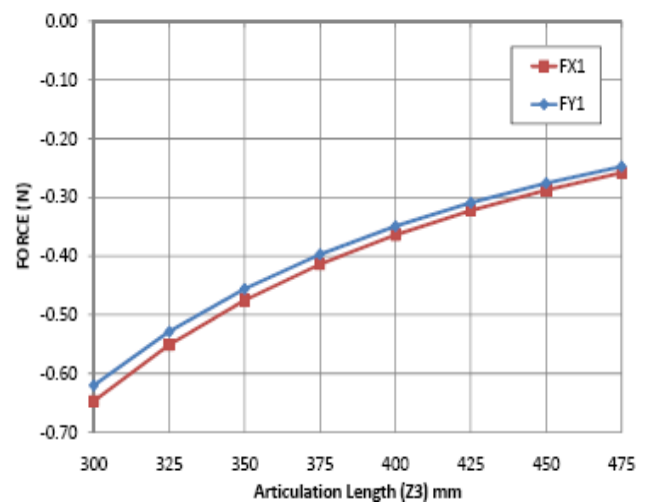


Fig 8. Articulation length Vs Forces

3.4 Parallel misalignment Vs Forces and moments

In this the induced Torque and bending stiffness and Articulation length are kept constant and with variation in Parallel misalignment of the HSFC, the resulting forces and moments are calculated for the typical HSFC is given in Table 5.

Table 5 Parallel misalignment Vs Forces and moments

Torque (Tq)	k_b	M_{X_1}	M_{Y_1}	M_{X_2}	M_{Y_2}	F_{X_1}	F_{Y_1}	ΔX_2	Z_3
100	4.75E+03	0	0	0.2353	11.176	-0.0263	0.0006	1	425
100	4.75E+03	0	0	0.7059	33.53	-0.0789	0.0017	3	425
100	4.75E+03	0	0	1.1765	55.884	-0.1315	0.0028	5	425
100	4.75E+03	0	0	1.6471	78.239	-0.1841	0.0039	7	425
100	4.75E+03	0	0	2.1176	100.6	-0.2367	0.0050	9	425
100	4.75E+03	0	0	2.5882	122.95	-0.2893	0.0061	11	425
100	4.75E+03	0	0	3.0588	145.32	-0.3419	0.0072	13	425
100	4.75E+03	0	0	3.5294	167.68	-0.3945	0.0083	15	425

The parallel misalignment Vs Forces and bending stiffness Vs moments are shown in Fig 9 & 10.

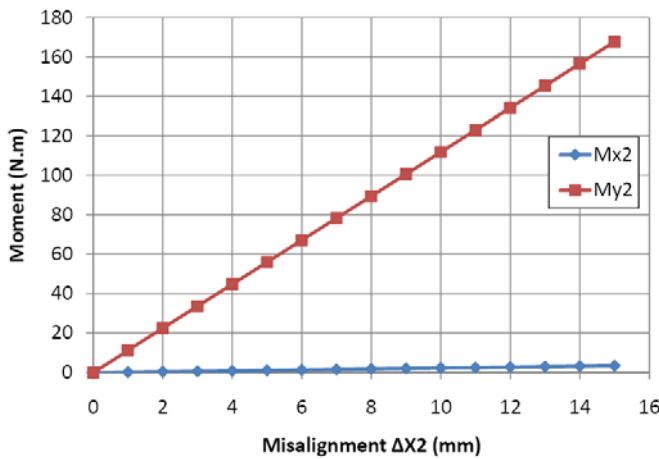


Fig 9. Parallel misalignment Vs end moments

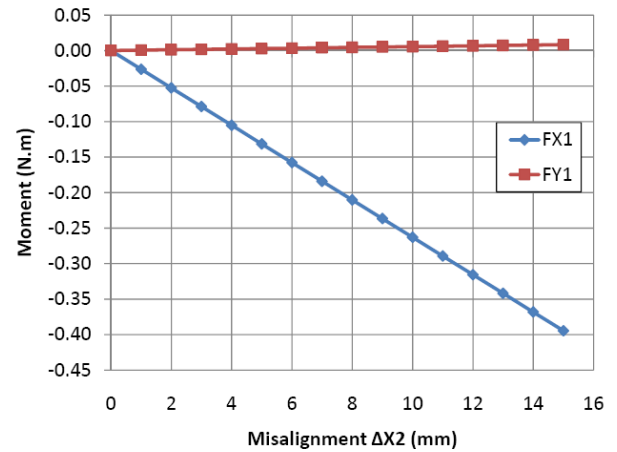


Fig 10. Parallel misalignment Vs Forces

3.5 Parallel misalignments in different planes Vs Forces and moments

In this the induced torques, bending stiffness and articulation lengths are kept constant, with the variation in parallel misalignments in different planes viz. ΔX_2 and ΔY_2 of the typical HSFC and the resulting forces and moments are found. The results are given in Table 6.

Table 6 Parallel misalignments in different planes Vs Forces and moments

Torque (Tq)	k_b	M_{X_1}	M_{Y_1}	M_{X_2}	M_{Y_2}	F_{X_1}	F_{Y_1}	ΔX_2	ΔY_2	Z_3
100	4.75E+03	0	0	-10.9412	11.412	-0.0269	-0.0257	1	1	425
100	4.75E+03	0	0	-32.8238	34.236	-0.0806	-0.0772	3	3	425
100	4.75E+03	0	0	-54.7072	57.06	-0.1343	-0.1287	5	5	425
100	4.75E+03	0	0	-76.5918	79.886	-0.1880	-0.1802	7	7	425
100	4.75E+03	0	0	-98.4781	102.71	-0.2417	-0.2317	9	9	425
100	4.75E+03	0	0	-120.3667	125.54	-0.2954	-0.2832	11	11	425
100	4.75E+03	0	0	-142.2580	148.38	-0.3491	-0.3347	13	13	425
100	4.75E+03	0	0	-164.1525	171.21	-0.4029	-0.3862	15	15	425

With the variation in parallel misalignments in ΔX_2 and ΔY_2 the increase in moments and reaction forces are observed. The Fig 11 & 12 shows the parallel misalignments induced in different planes Vs forces and bending moments.

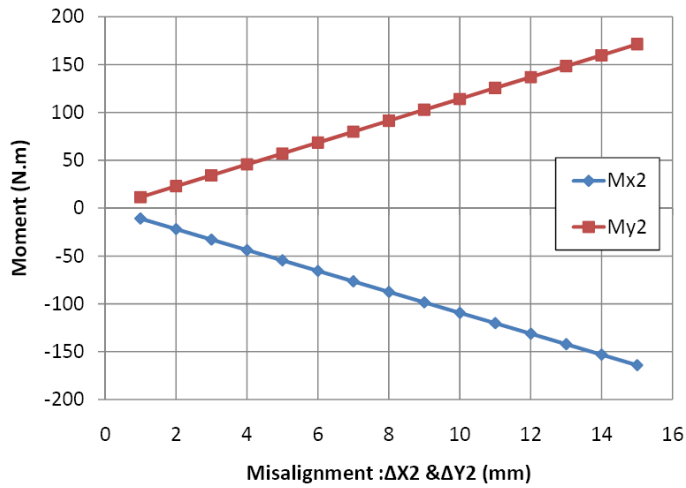


Fig 11. Parallel misalignment in different planes Vs end moments

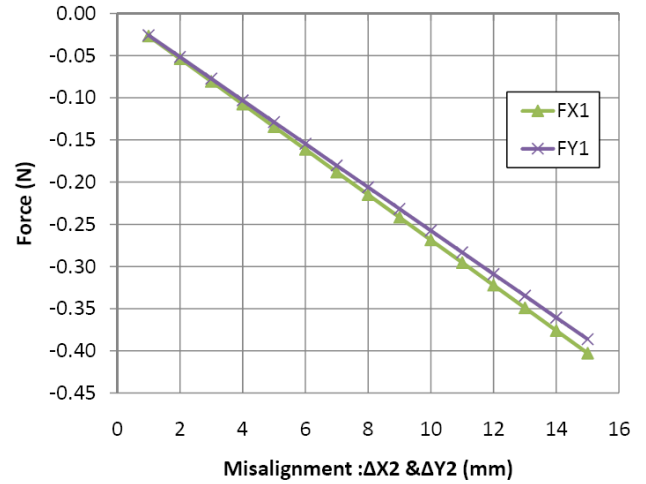


Fig 12. Parallel misalignment in different planes Vs Forces

4. Axial misalignment

The Axial misalignment of HSFC assembly can be modeled as springs connected in parallel. The HSFC has two flexible plates pack which are acts as springs connected in a parallel manner by centre tube. As the flexible plates pack are in parallel the absolute deflection is equal to the deflection of the system and each flexible plates pack is carrying part of the total load applied such that the total load supported is equal to the sum of the loads carried by individual springs. In present case flexible plates may be considered as spring 1 and spring 2 with axial stiffness of K_1 and K_2 respectively as shown in Fig 13. The equivalent axial spring rate is given by eq (16). The axial misalignment (X_a) imposed on the HSFC resulting in the reaction force (F) at the supporting end is given by eq (17).

$$K_a = K_1 + K_2 \quad (16)$$

$$F = K_a \cdot X_a \quad (17)$$

The axial misalignment (imposed on the HSFC and resulting forces (F) at the supporting end are shown in Fig.14. The linear spring rates for the HSFC in axial mode is assumed.

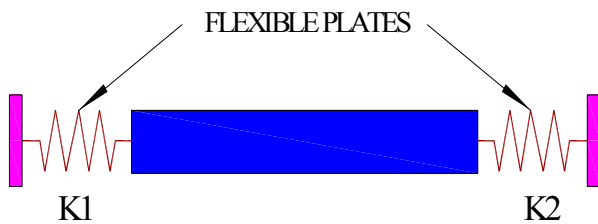


Fig 13. Axial misalignment of HSFC

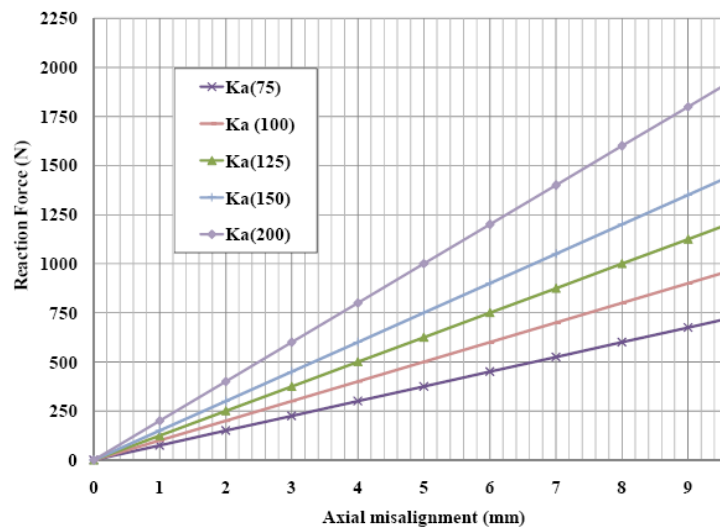


Fig 14. Axial misalignment of HSFC Vs Reaction forces

From the results it is shown that the axial misalignment governed by the axial stiffness of HSFC and lower axial stiffness will be resulting in minimal reaction forces.

5. Experimental validation of axial misalignment

The reaction forces during axial misalignment of the typical HSFC are validated by axial thrust test rig as shown in Fig 15. The Axial thrust test rig comprises of two mounting flanges for accommodating the test unit. In this, one flange is fixed and other one is movable by the motion imparted by a lead screw and a turning hand wheel arrangement. The extension length is measured in steps of 0.5 mm by the dial gauge, attached to the structure. The deflection of test unit on extension is measured by the dial gauge and load due to extension is measured by load cell provided on fixed mounting flange. The typical HSFC assembly is subjected to maximum axial misalignment of 2.5 mm in steps of 0.5 mm and after completion of the test, the assembly was visually examined and that no evidence of failure and yielding was found. The reaction forces measured are closely agrees with the theoretical predications. The theoretical prediction Vs model behavior of HSFC is shown in Fig 16.



Fig 15. Axial thrust test rig

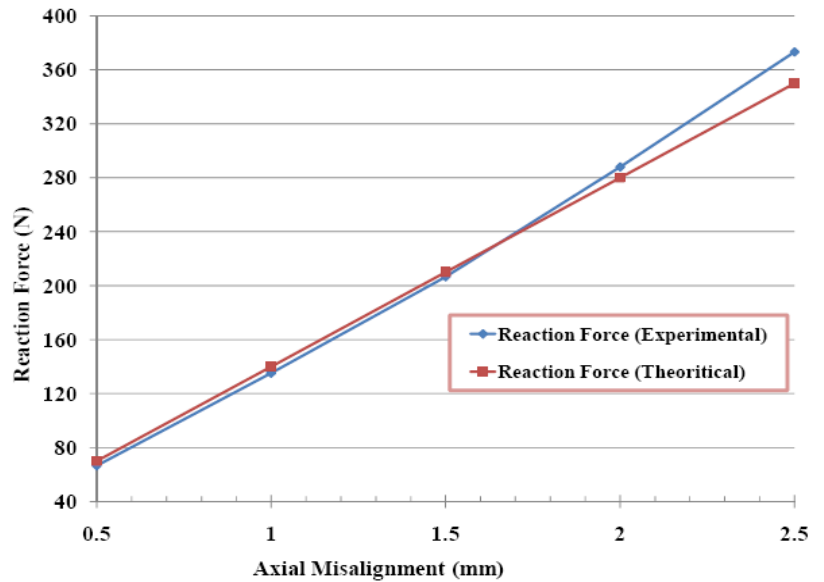


Fig 16. Theoretical prediction Vs Model behavior

5.1 Combined axial and parallel misalignment test of HSFC

The typical HSFC developed has been subjected to extensive testing in combined axial and parallel misalignment for 10 million cycles at 12000 rpm. The misalignment cycle test rig as shown in Fig 17. The objective of this test is to check and verify the satisfactory endurance performance of typical HSFC. The test rig is configured with a DC motor and a, step up gearbox along with a torque speed sensor. The axial and parallel misalignment of the High speed flexible coupling can be imposed with a special cross table screw arrangement at the drive end.

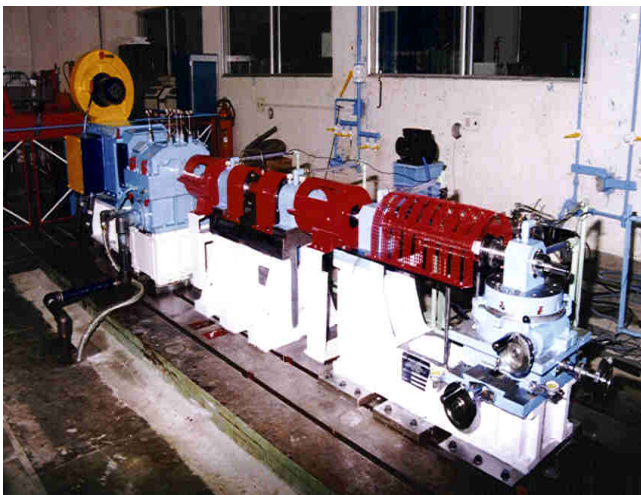


Fig 17. Misalignment cycle test rig

Table 7 Combined axial and parallel misalignment test conditions of HSFC

Sl. No	Speed (rpm)	Parallel misalignment (mm)	Axial misalignment (mm)	Cycles (revolutions)
1	12000	0.3	0.5	10 million
2	12000	0.6	1.0	10 million
3	12000	0.9	1.5	10 million
4	12000	1.2	2.0	10 million
5	12000	1.5	2.5	10 million
6	12000	1.85	2.5	10 million

The HSFC assembly was mounted and drive end flange is imposed with equivalent parallel and axial misalignment. During testing, speed, vibrations at the input and the output ends and noise level are monitored and recorded. The axial misalignment up to 2.5 mm and parallel misalignment up to 1.85 mm was imposed. For each load step, the testing was conducted for 10 million cycles. After completion of the test, the HSFC assembly was visually examined and found no evidence of failure and yielding which shows that the bending moments and reaction forces are well within the acceptable limits.

6. Discussion

The effect of various misalignment of HSFC on the Fighter aircraft transmission characteristics has been analyzed. The articulation length of the HSFC influences the parallel misalignment accommodating capability of HSFC. The analysis performed clearly shows that as the articulation length of the coupling increases the corresponding moment and forces on the end support are decreasing. Hence it is advantageous to place the flexible plate packs as closer to the support ends as the corresponding bending stress induced on the flexible elements will be less thereby increase in the HSFC service life. The HSFC's bending stiffness to be designed as lowest as possible. The increase in parallel misalignment in multiple planes will result in increase in support end forces and bending moments. This has to be carefully studied for the rating of HSFC parallel misalignment capability. During installation care to be taken to align the HSFC to reduce the static misalignment. The axial misalignment governed by the axial stiffness of HSFC and with lower axial stiffness the corresponding reaction forces will be minimum. From the experimental evaluation of forces due to axial misalignment, minor variation in theoretical prediction Vs model behavior is observed. This is may be due to the friction present in the test set up. The successful performance of HSFC in combined axial and parallel misalignment test indicates that the bending moments and reaction forces are well within the acceptable limits. The suitability of the model adapted for the design iteration of HSFC has been successfully implemented.

7. Conclusion

In the present study, influence of articulation length and effect of reaction force and moments experienced by the coupling has been carried out. The coupling misalignment forces and moments have been determined for both parallel and angular misalignments of a HSFC. It is observed that the coupling can be designed to accommodate more parallel misalignment by positioning the flexible elements with optimized articulation length. The axial misalignment capability of the shaft is sole function of axial stiffness of the flexible elements. This observation will be useful in designing of compact flexible coupling where higher misalignment capability within the available space has to be met. With the experimentation, the suitability of the model adapted for the design iteration of HSFC development is validated. This method will reduce the design iteration cycles of HSFC and can be extended for the similar development of flexible couplings.

Nomenclature

FX_1	forces in X1 direction, [N]	Tq	torque , [N-mm]
FX_2	forces in X2 direction, [N]	Xa	axial misalignment, [mm]
FY_1	forces in Y1 direction, [N]	Z_3	articulation length, [mm]
FY_2	forces in Y2 direction, [N]	θ_1	Rotating angle in X_1 direction, [deg]
K_a	axial stiffness, [N/mm]	θ_2	Rotating angle in X_2 direction ,[deg]
Kb	bending stiffness, [N.mm/deg]	θ_3	misalignment angle, [deg]
Ke	equivalent axial stiffness of flexible plate packs, [N/mm]	Φ_1	Rotating angle in Y_1 direction, [deg]
K_1, K_2	axial stiffness of Flexible plate packs, [N/mm]	Φ_2	Rotating angle in Y_2 direction,[deg]
MX_1	moments in X_1 direction, [N-mm]	ΔX_1	misalignment displacement on X_1 direction, [mm]
MX_2	moments in X_2 direction, [N-mm]	ΔX_2	misalignment displacement on X_2 direction, [mm]
MY_1	moments in Y_1 direction, [N-mm]	ΔY_1	misalignment displacement on Y_1 direction, [mm]
MY_2	moments in Y_2 direction, [N-mm]	ΔY_2	misalignment displacement on Y_2 direction ,[mm]

References

- [1] Nagesh.S., Ganesan.S. and Chandra sekaran C., 2004, "Design and Development of Power take off shaft with contoured diaphragms for Aircraft applications DRDO work shop on advanced manufacturing," DRDL, Hyderabad, pp. 784-794.
- [2] ANSI/AGMA 9009-D02: "Flexible Couplings- Nomenclature for Flexible Couplings".
- [3] Agnieszka Muszynska, 2005, "Rotor dynamics," CRC Press Taylor & Francis Group.
- [4] C.B.Gibbons, 1976, "Coupling misalignment forces," Proceedings of the Fifth Turbo machinery Symposium Gas Turbine Laboratories\ Texas A & M University, College Station, Texas, pp. 111-116.
- [5] A.S. Sekhar and B.S. Prabhu, 1995, "Effects of coupling misalignment on vibrations of rotating machinery," Journal of Sound and Vibration, Vol. 185 (4), pp. 655-671.
- [6] Nagesh S., 2000, "Lateral critical speed analysis of high speed shaft with contoured diaphragms using transfer matrix Method," M.E. thesis, PSG college of Technology, Coimbatore.